Ductile Fe-Based BMGs with High Glass Forming Ability and High Strength

Fengjuan Liu, Quanwen Yang, Shujie Pang, Chaoli Ma and Tao Zhang*

Department of Materials Science and Engineering, Beijing University of Aeronautics and Astronautics, Beijing 100083, P. R. China

Fe-based bulk metallic glasses (BMGs) with high glass forming ability (GFA) and excellent mechanical properties were synthesized in Fe-Ni-Mo-P-C-B alloy system by copper mold casting. Results show that the glass forming ability of $Fe_{74-x}Ni_xMo_6P_{10}C_{7.5}B_{2.5}$ alloys increases first and then decreases as Ni content, x, increases from 0 to 11.1 at%, with its climax being reached at x is between 3.7 and 5.0. Analyses indicate that either ΔT_x and ΔH_{endo} or T_{rg} and γ can not illustrate the GFA of obtained alloys solely. With increasing Ni element in $Fe_{74-x}Ni_xMo_6P_{10}C_{7.5}B_{2.5}$ alloys, the yield strength and Vicker's mircohardness decline, while the plasticity increases, which implies that enhancing plasticity by adjusting the composition of alloys is followed with the loss of some strength. Serrated flow characteristics on the compressive stress-strain curves is observed for $Fe_{74-x}Ni_xMo_6P_{10}C_{7.5}B_{2.5}$ as $x = 11.1$ at%, which is considered to relate to its lowest glass transition temperature. These mechanical properties of BMGs are illustrated with bonding nature between the constituent elements.   [doi:10.2320/matertrans.MRA2007186]

1. Introduction

Since Fe-based bulk metallic glass (BMG) was synthesized by copper mold casting for the first time in 1995,[1] a variety of Fe-based BMGs with high GFA and good magnetic properties have been developed for the potential magnetic applications.[2–5] However, for being utilized directly in bulk form in magnetic devices, such as magnetic sensors, valves or clutches, the Fe-based BMGs should also present high mechanical strength and good ductility besides good soft magnetic properties. Mechanical properties of bulk Fe-based glasses have absorbed researcher's interest in the recent years.[6–13] Although most Fe-based BMGs are reported to possess high strength over 3 GPa, their plastic strain is usually less than 0.5%[6–12] except for a plastic strain of 1.9% for Fe-Nb-Si-B.[13] Recently, we have reported Fe-Mo-P-C-B BMG with diameter of 2 mm combined with larger plastic strain and good soft magnetic properties.[14] To synthesize Fe-based BMGs with higher GFA and more excellent ductility, we tried to substitute part of Fe with Ni in Fe-Mo-P-C-B alloy system, basing on the consideration that nickel is soft and has ever been successfully substituted for Fe to enhance the GFA of Fe-based BMGs.[12] As a result, Fe-based BMGs with diameter up to 5 mm and plastic strain up to 4% are synthesized in $Fe_{74-x}Ni_xMo_6P_{10}C_{7.5}B_{2.5}$ alloy system. In this paper, we will investigate how the GFA and mechanical properties varying with Ni content, and the relations of the serrated flow characteristic on the compressive stress-strain curves with the glass transition temperature of glassy alloys.

2. Experimental Procedure

Alloy ingots of $Fe_{74-x}Ni_xMo_6P_{10}C_{7.5}B_{2.5}$ ($x = 0 - 14.8$ at%) were prepared by induction melting the mixtures of pure Fe (99.9 mass%), Ni (99.9 mass%), Mo (99.9 mass%), C (99.9 mass%) and B (99.9 mass%), and pre-alloyed Fe-P ingots under a high-purity argon atmosphere. From the master alloys, ribbons were prepared by single-roller melt-spinning and cylindrical rods with diameters from 1 to 6 mm

were produced by copper mold casting. Structures of ribbons and the transverse cross sections of the rods were examined by X-ray diffractometry (XRD) with Cu-$K\alpha$ radiation and high-resolution transmission electron microscopy (HRTEM). Thin foil specimens for HRTEM observations were prepared by ion-beam milling with a liquid nitrogen-cooled stage. Thermal stability associated with the glass transition temperature (T_g), crystallization temperature (T_x), supercooled liquid region ($\Delta T_x = T_x - T_g$), enthalpy of supercooled liquid (ΔH_{endo}), melting temperature (T_m) and liquid (T_l) temperature, was examined by differential scanning calorimetry (DSC) at a heating rate of 0.33 K/s. Compressive tests were performed on a material test system (MTS) at a strain rate of $2.1 \times 10^{-4}\,s^{-1}$ at room temperature using as-cast glassy rods with a dimension of 1 mm in diameter and 2 mm in length. Deformation and fracture behaviors were examined by scanning electron microscopy (SEM). Microhardness was determined by a Vickers hardness indenter with a load of 200 g. Magnetic property of saturation magnetization (B_s) was measured with a vibrating sample magnetometer (VSM) under an applied field of 800 kA/m.

3. Results

Cylindrical glassy alloy rods with diameters up to 5 mm were formed in the $Fe_{74-x}Ni_xMo_6P_{10}C_{7.5}B_{2.5}$ alloy system in the range of $x = 0 - 14.8$ at% by copper mold casting, although crystalline phases were found in the 2 mm-diameter rods for the alloys containing 14.8 at% Ni. X-ray diffraction patterns of the $Fe_{74-x}Ni_xMo_6P_{10}C_{7.5}B_{2.5}$ ($x = 0, 3.7, 5, 7.4, 11.1$ at%) glassy alloy rods in critical diameters (3, 5, 5, 4, 3 mm, respectively) for glass formation are shown in Fig. 1. Only broad smooth peaks on the curves indicate the absence of a crystalline phase in the specimens at the sensitivity of XRD. Glassy structures of the bulk samples are further confirmed with HRTEM examinations and comparisons of the DSC curves between the ribbon and bulk samples. As one example, DSC curves of the $Fe_{69}Ni_5Mo_6P_{10}C_{7.5}B_{2.5}$ alloy rods of 1 mm and 5 mm in diameter and that of the glassy ribbon are shown in Fig. 2. No appreciable differences in T_g, T_x and total heat release of the crystallization peaks (ΔH_x)

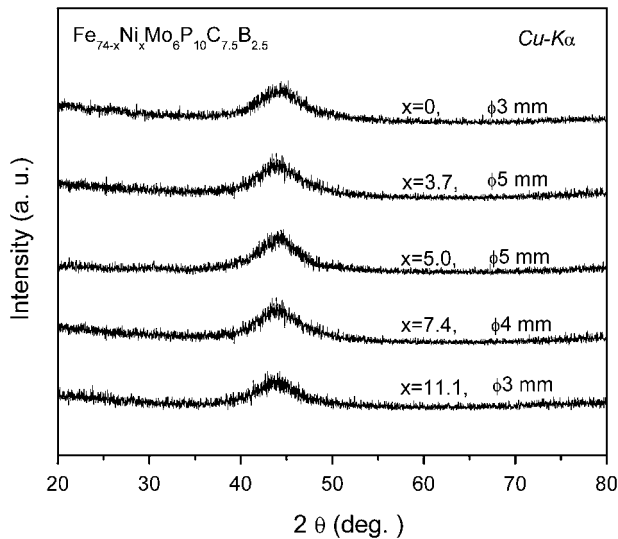*Corresponding author, E-mail: zhangtao@buaa.edu.cn

Fig. 1 X-ray diffraction patterns of $Fe_{74-x}Ni_xMo_6P_{10}C_{7.5}B_{2.5}$ ($x = 0 - 11.1$ at%) glassy alloy rods with their critical diameters for glass formation.
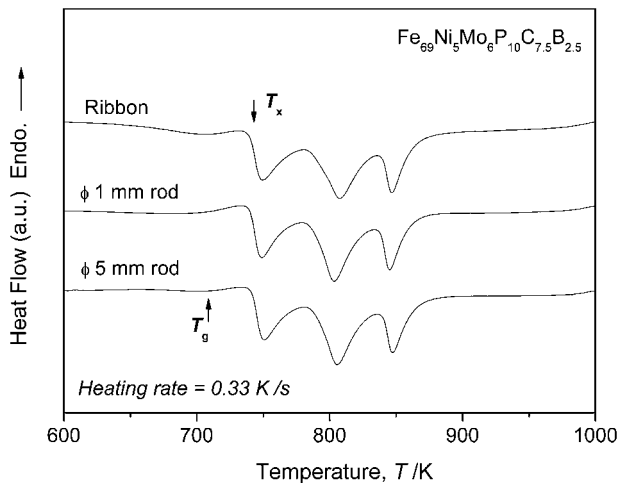

Fig. 2 DSC curves of $Fe_{69}Ni_5Mo_6P_{10}C_{7.5}B_{2.5}$ alloy ribbon and rods with diameters of 1 and 5 mm.

Fig. 3 High-resolution transmission electron micrograph (a) and selected-area electron diffraction pattern (b) of the cast $Fe_{69}Ni_5Mo_6P_{10}C_{7.5}B_{2.5}$ alloy rod with a diameter of 5 mm.

Fig. 4 DSC curves of the bulk $Fe_{74-x}Ni_xMo_6P_{10}C_{7.5}B_{2.5}$ ($x = 0, 3.7, 5.0, 7.4, 11.1$ at%) glassy alloys with 2 mm-diameter rods.

can be recognized, indicating they have the similar glassy structure. The HRTEM examinations on the 5 mm rod of $Fe_{69}Ni_5Mo_6P_{10}C_{7.5}B_{2.5}$ alloy show that the dark-field transmission electron micrograph (Fig. 3(a)) is featureless and the selected area electron diffraction (SAED) pattern (Fig. 3(b)) consists only of halo rings, which is inherent for amorphous phase.

DSC curves of the bulk $Fe_{74-x}Ni_xMo_6P_{10}C_{7.5}B_{2.5}$ ($x = 0, 3.7, 5.0, 7.4, 11.1$ at%) glassy alloys with 2 mm-diameter rods are shown in Fig. 4. It can be seen from the curves that all of these alloys exhibit a distinct glass transition followed by crystallization and melting. The T_g, T_x, ΔT_x and ΔH_{endo} (indicated by area of endothermic peak of supercooled liquid) of the $Fe_{74}Mo_6P_{10}C_{7.5}B_{2.5}$ alloy are 711 K, 749 K, 38 K and 2.02 J/g, respectively. ΔH_{endo} is defined as an integration of enthalpy difference between glassy solid and supercooled liquid by temperature range from T_g to T_x. It may be considered that thermal stability of the supercooled liquid
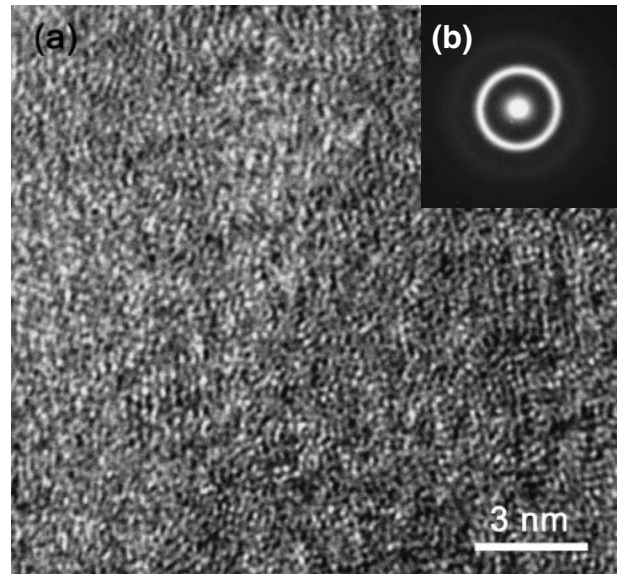
against crystallization increases with increasing ΔH_{endo}. For the glassy alloys with Ni content of 3.7–11.1 at%, T_g and T_x decrease from 713 to 698 K and from 747 to 739 K, respectively, and ΔT_x and ΔH_{endo} increase from 34 to 41 K and from 2.7 to 5.75 J/g, respectively. Larger ΔT_x and ΔH_{endo} could be regarded as an indicator of higher GFA of alloys[15–17] for their implication of greater capability against nucleation and growth of crystalline for super-cooled liquid, therefore, value trends of above ΔT_x and ΔH_{endo} might
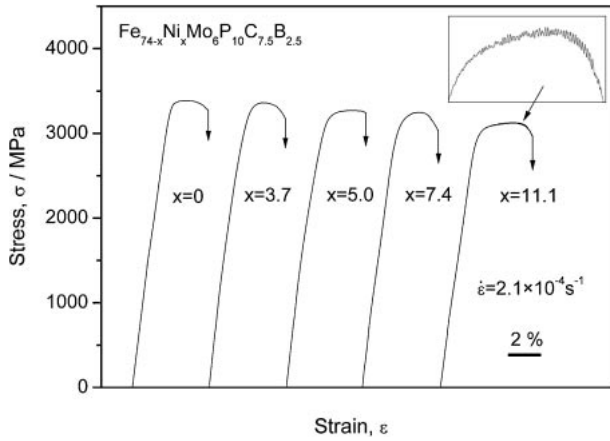
Fig. 5 Compressive stress-strain curves of bulk glassy $Fe_{74-x}Ni_xMo_6P_{10}C_{7.5}B_{2.5}$ ($x = 0, 3.7, 5.0, 7.4, 11.1$ at%) rods with a diameter of 2 mm, inserted with local magnified curve for the alloy with 11.1 at% Ni.

Fig. 6 Hysteresis B-H curves of $Fe_{74-x}Ni_xMo_6P_{10}C_{7.5}B_{2.5}$ ($x = 0, 3.7, 5.0, 7.4, 11.1$ at%) glassy ribbons.

indicate that the GFA of the alloys increase with increasing Ni. Further more, as shown in Fig. 4, for $Fe_{74-x}Ni_xMo_6P_{10}C_{7.5}B_{2.5}$ alloys with Ni content increasing from 0 to 11.1 at%, T_m decreases from 1208 to 1179 K and T_l increases from 1255 to 1335 K, which results in the reduced glass transition temperature T_{rg} (T_g/T_l) decreases from 0.57 to 0.52 and γ defined as $T_x/(T_g + T_l)$ decreases from 0.381 to 0.364. High T_{rg} and γ are also representative criteria of relatively high GFA.[18,19] The decrease of T_{rg} and γ might indicate that the GFA of the alloys decrease with increasing Ni content. From these experimental results, we know that the glass forming ability of $Fe_{74-x}Ni_xMo_6P_{10}C_{7.5}B_{2.5}$ alloys increases first and then decreases as Ni content, x, increases from 0 to 11.1 at%, with its climax being reached at x that is between 3.7 and 5.0. This phenomenon shows that either ΔT_x and ΔH_{endo} or T_{rg} and γ can not illustrate the GFA of present glassy alloys solely. The maximum GFA obtained at certain element content is in agreement with our previous simulation results.[20] That is to say, the non-crystalline structures may have the largest growth rate during rapid solidification for $Fe_{74-x}Ni_xMo_6P_{10}C_{7.5}B_{2.5}$ alloys with Ni content between 3.7 and 5.0, which result in the highest GFA of these alloys.

Further investigations on the mechanical properties of present Fe-based BMGs show that they vary regularly with increasing Ni element. Compressive stress-strain curves of the $Fe_{74-x}Ni_xMo_6P_{10}C_{7.5}B_{2.5}$ ($x = 0, 3.7, 5.0, 7.4, 11.1$ at%) glassy alloys are shown in Fig. 5, inserted with local magnified curve for the alloy with 11.1 at% Ni. It can be seen that the alloys exhibit obvious elastic strain, followed by large plastic strain before fracture. With Ni content, x, increasing from 0 to 11.1, the plastic strain increases from 2.2% to 4.0%, while the yield strength and fracture strength decrease from 3330 to 2780 MPa, and from 3400 to 3120 MPa, respectively, which implies that enhancing plasticity by adjusting the composition of alloys is followed with the loss of some strength. Similar to the Fe-Mo-P-C-B alloy system,[14] the large plasticity of present alloys attributes to high density of shear bands formed during compression. The fracture surface exhibits a typical vein pattern, which is the characteristic of ductile feature of BMGs.
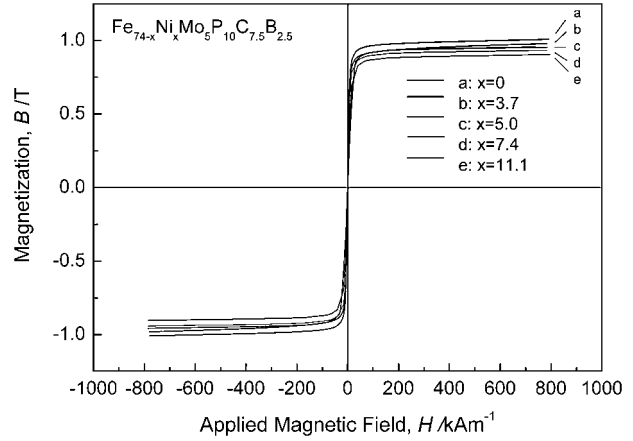
Besides high strength and large plastic strain, high microhardness and good soft magnetic properties are also achieved by $Fe_{74-x}Ni_xMo_6P_{10}C_{7.5}B_{2.5}$ ($x = 0, 3.7, 5.0, 7.4, 11.1$ at%) alloys. The microhardness decreases from 1060 to 890 for these alloys as their Ni content varies from 0 to 11.1 at%. Magnetic properties can be illustrated by the hysteresis B-H curves of these alloys in ribbons as shown in Fig. 6. We can see from the curves that these alloys achieve good soft magnetic properties represented by low coercive force and high permeability. Their saturation magnetization (B_s) decreases slightly from 1.02 to 0.9 T as Ni content increases from 0 to 11.1 at%.

4. Discussion

From above results, we know that the alloys' mechanical properties change with Ni element content regularly. For example, the plasticity of present Fe-based glassy alloys is enhanced by increasing Ni element, the addition of which also results in the loss of strength. These effects are considered to relate to the bonding nature among the constituent elements atoms of alloys. The weaker bonding nature implies lower energy barrier for atom diffusion and decreased viscosity of alloys, and makes the atoms much easier to rearrange, which results in enhanced ductility and decreased yield strength. For the Fe-Ni-Mo-P-C-B BMGs, the bonding in them might become weaker by partial substitution of transition element of Ni for Fe. This effect can be understood with three viewpoints, i.e., the electrons transferring between the constituent elements, mixing enthalpy of the atomic pairs, and the glass transition temperature of glassy alloys, which are discussed respectively in detail below.

Chen et al.[21,22] have pointed out that an s-d hybrid bonding could form by electrons transferring from the metalloid elements, such as P and B, to fill the d shells in the transition metal elements, such as Fe and Ni. The numbers of 3d band electrons in Fe is 6, while that of Ni is 8, so that the fraction of empty shell of 3d band will be reduced for the substitution of Ni for Fe in our alloys. The number of s-d hybrid bonding will decrease for reduction of empty shell of 3d band, which results in the weaker bonding between

atoms in alloys. Therefore, we can deduce that bonding nature in our alloys should be reduced for increasing Ni content.

The bonding nature among the constituent elements could also be illustrated with the mixing enthalpies of the atomic pairs. The mixing enthalpies of Fe-P, Fe-B, and Fe-C atomic pairs are -41, -11, $40\,\mathrm{kJ/mol}$, respectively, and that of Ni-P, Ni-B, and Ni-C atomic pairs are -26, -9, $51\,\mathrm{kJ/mol}$, respectively.[23] It is noticeable that the mixing enthalpies of atomic pairs with Fe element are more negative than those of atomic pairs with Ni element. The more negative mixing enthalpy indicates the stronger atomic interaction, therefore, the substitution of Fe with Ni in present alloy system is assumed to weaken the bonding between the constituent elements.

Lower T_g is also a denotation of weak atomic interaction, so that it has the same trend as bonding nature, and we assume that glassy alloys with lower T_g correspond to weaker bonding nature. In our present Fe-Ni-Mo-P-C-B alloy with increasing Ni element, T_g decreases from 713 K to 698 K, which is in agreement with the depression of strength. The same trend of bonding nature and T_g is further validated by the evident serrated flow characteristic on the compressive stress-strain curve of glassy alloy as Ni content increases to 11.1 at% (as shown in Fig. 4). Wei et al.[24] found that serrated flow characteristic on the load-displacement curves of BMGs during nanoindentation related tightly to the T_g. Johnson et al.[25] deduced that lower T_g related to depressed plastic yielding of metallic alloys, and Wang et al.[26] have also suggested that BMGs with T_g close to room temperature are prone to exhibit room temperature ductility. These results agree well with our assumption.

5. Conclusions

Bulk metallic glasses with critical diameters up to 5 mm were synthesized in Fe-Ni-Mo-P-C-B system by copper mold casting. Analyses indicate that either ΔT_x and ΔH_{endo} or T_{rg} and γ can not be used to illustrate the GFA of obtained alloys solely. With increasing Ni element in $Fe_{74-x}Ni_xMo_6P_{10}C_{7.5}B_{2.5}$ alloys, the plasticity increases, while the yield strength and Vicker's mircrohardness decline, which implies that enhancing plasticity by adjusting the composition of alloys is followed with the loss of some strength. Serrated flow of compressive stress-strain curves, indicating ductile characteristic of alloy, are found to be more obvious as Ni content reaches at 11.1 at% and T_g decreases to 698 K in present alloy system. The regular mechanical properties of obtained BMGs with increasing Ni element are illustrated by the bonding nature between the constituent elements. The comprehensive excellent properties of these Fe-based ferromagnetic bulk glassy alloys imply their extensive application as new structural and functional materials.

REFERENCES

1) A. Inoue, Y. Shinohara and J. S. Gook: Mater. Trans., JIM **36** (1995) 1427–1433.
2) T. D. Shen and R. B. Schwarz: Appl. Phys. Lett. **75** (1999) 49.
3) A. Inoue, A. Takeuchi and B. L. Shen: Mater. Trans. **42** (2001) 970–978.
4) B. L. Shen and A. Inoue: Mater. Trans. **43** (2002) 1235–1239.
5) A. Inoue and K. Hashimoto: *Amorphous and Nanocrystalline Materials: Preparation, Properties, and Applications*, (Berlin, 2001) pp. 34–38.
6) V. Ponnambalam, S. J. Poon and G. J. Shiflet: J. Mater. Res. **19** (2004) 1320–1323.
7) Z. P. Lu, C. T. Liu, J. R. Thomson and W. D. Porter: Phys. Rev. Lett. **92** (2004) 245503.
8) M. Stoica, K. Hajlaoui, A. LeMoulec and A. R. Yavari: Phil. Mag. Lett. **86** (2006) 267–275.
9) B. L. Shen and A. Inoue: Appl. Phys. Lett. **85** (2004) 4911.
10) A. Inoue, B. L. Shen, A. R. Yavari and A. L. Greer: J. Mater. Res. **18** (2004) 1487–1492.
11) X. J. Gu, A. G. McDermott, S. J. Poon and G. J. Shiflet: Appl. Phys. Lett. **88** (2006) 211905.
12) C. T. Chang, B. L. Shen and A. Inoue: Appl. Phys. Lett. **89** (2006) 051912.
13) K. Amiya, A. Urata, N. Nishiyama and A. Inoue: Mater. Trans., JIM **45** (2004) 1214–1218.
14) T. Zhang, F. J. Liu, S. J. Pang and R. Li: Mater. Trans. **48** (2007) 1157–1160.
15) A. Inoue, T. Zhang and T. Masumoto: J. Non-Cryst. Solids **156–158** (1997) 473–480.
16) Y. Li, S. N. Ng and C. K. Ong, *et al.*: Scripta Mater. **36** (1997) 783–787.
17) B. L. Shen, C. T. Chang, T. Kubota and A. Inoue: J. Appl. Phys. **100** (2006) 013515.
18) Z. P. Lu and C. T. Liu: Acta Mater. **50** (2002) 3501–3512.
19) Z. P. Lu and C. T. Liu: Phys. Rev. Lett. **91** (2003) 115505.
20) Q. W. Yang and T. Zhang: J. Phys.: Condens. Matt. **19** (2007) 086212.
21) H. S. Chen, J. T. Krause and E. Coleman: J. Non-Cryst. Solids **18** (1975) 157–171.
22) B. L. Shen, M. Akiba and A. Inoue: J. Appl. Phys. **100** (2006) 043523.
23) F. R. De Boer, R. Boom, W. C. M. Mattens, A. R. Miedema and A. K. Niessen: *Cohesions in Metals*, (North-Holland, Amsterdam, The Netherlands, 1989).
24) W. H. Li, B. C. Wei, T. H. Zhang, D. M. Xing, L. C. Zhang and Y. R. Wang: Intermetallics **15** Issues 5–6 (2007) 706–710.
25) W. L. Johnson and K. Samwer: Phys. Rev. Lett. **95** (2005) 195501.
26) B. Zhang, D. Q. Zhao, M. X. Pan, W. H. Wang and A. L. Greer: Phys. Rev. Lett. **94** (2005) 205502.